Behavioral/Systems/Cognitive

cGMP Produced by NO-Sensitive Guanylyl Cyclase Essentially Contributes to Inflammatory and Neuropathic Pain by Using Targets Different from cGMP-Dependent Protein Kinase I

Achim Schmidtko,[1] Wei Gao,[1] Peter König,[2] Sandra Heine,[1] Roberto Motterlini,[3] Peter Ruth,[4] Jens Schlossmann,[5] Doris Koesling,[6] Ellen Niederberger,[1] Irmgard Tegeder,[1] Andreas Friebe,[6] and Gerd Geisslinger[1]

[1]Pharmazentrum Frankfurt/ZAFES, Institut für Klinische Pharmakologie, Klinikum der Johann Wolfgang Goethe-Universität, 60590 Frankfurt am Main, Germany, [2]Institut für Anatomie, Universität zu Lübeck, 23538 Lübeck, Germany, [3]Department of Surgical Research, Northwick Park Institute for Medical Research, Harrow HA1 3UJ, Middlesex, United Kingdom, [4]Pharmakologie und Toxikologie, Pharmazeutisches Institut, 72076 Tübingen, Germany, [5]Institut für Pharmakologie und Toxikologie, Universität Regensburg, 93040 Regensburg, Germany, and [6]Medizinische Fakultät, Institut für Pharmakologie und Toxikologie, Ruhr-Universität Bochum, 44780 Bochum, Germany

A large body of evidence indicates that the release of nitric oxide (NO) is crucial for the central sensitization of pain pathways during both inflammatory and neuropathic pain. Here, we investigated the distribution of NO-sensitive guanylyl cyclase (NO-GC) in the spinal cord and in dorsal root ganglia, and we characterized the nociceptive behavior of mice deficient in NO-GC (GC-KO mice). We show that NO-GC is distinctly expressed in neurons of the mouse dorsal horn, whereas its distribution in dorsal root ganglia is restricted to non-neuronal cells. GC-KO mice exhibited a considerably reduced nociceptive behavior in models of inflammatory or neuropathic pain, but their responses to acute pain were not impaired. Moreover, GC-KO mice failed to develop pain sensitization induced by intrathecal administration of drugs releasing NO or carbon monoxide. Surprisingly, during spinal nociceptive processing, cGMP produced by NO-GC may activate signaling pathways different from cGMP-dependent protein kinase I (cGKI), whereas cGKI can be activated by natriuretic peptide receptor-B dependent cGMP production. Together, our results provide evidence that NO-GC is crucially involved in the central sensitization of pain pathways during inflammatory and neuropathic pain.

Key words: **nitric oxide; natriuretic peptide; spinal cord; DRG; knock-out mice; pain behavior**

Introduction

An exaggerated pain sensitivity is the dominant feature of inflammatory and neuropathic pain both in the clinical setting and in experimental animal models. It manifests as pain in response to normally innocuous stimuli (allodynia), increased response to noxious stimuli (hyperalgesia), or spontaneous pain, and can persist long after the initial injury is resolved (Scholz and Woolf, 2002; Woolf, 2004). The release of nitric oxide (NO) within the spinal cord has long been implicated in the mechanisms underlying exaggerated pain sensitivity (Meller and Gebhart, 1993). For example, a reduced nociceptive behavior was observed in several animal models of pain after intrathecal administration of NO synthase (NOS) inhibitors (Malmberg and Yaksh, 1993; Meller et al., 1994; Mabuchi et al., 2003) and after genetic deletion of the neuronal NOS (nNOS) isoform (Tao et al., 2004; Chu et al., 2005; Boettger et al., 2007). The essential contribution of NO for nociceptive processing was also demonstrated by recent electrophysiological experiments revealing that NO is necessary for the induction of long-term potentiation (LTP) of synaptic strength in spinal dorsal horn neurons that project to the periaqueductal gray (Ikeda et al., 2006).

NO signals by various mechanisms including cGMP synthesis, nitrosylation of ion channels, ADP-ribosylation, and the interaction with molecular oxygen and superoxide radicals to produce reactive nitrogen species that can modify a number of macromolecules (Davis et al., 2001). A major signaling mechanism of NO in spinal nociceptive processing initiates with activation of NO-sensitive guanylyl cyclase (NO-GC; also called soluble guanylyl cyclase) and subsequent cGMP production (Garry et al., 1994; Tao and Johns, 2002). It has been speculated that activation of cGMP-dependent protein kinase I (cGKI), in turn, is the major effector of NO-dependent cGMP synthesis in the spinal cord (Qian et al., 1996; Tao et al., 2000). However, although it is clear that nNOS and cGKI play an important role in spinal nociceptive processing, direct evidence for the presence of a functional NO/NO-GC/cGMP/cGKI pathway in this context is lacking.

Received May 9, 2008; revised July 3, 2008; accepted July 17, 2008.

This work was supported by Deutsche Forschungsgemeinschaft Grant DFG-SFB 553/C6 and Medizinische Fakultät der Universität zu Lübeck Grant A31–2007 (P.K.). We thank Inga Rauhmeier for excellent technical assistance.

Correspondence should be addressed to Dr. Achim Schmidtko, Pharmazentrum Frankfurt/ZAFES, Institut für Klinische Pharmakologie, Klinikum der Johann Wolfgang Goethe-Universität, Theodor-Stern-Kai 7, 60590 Frankfurt am Main, Germany. E-mail: Schmidtko@em.uni-frankfurt.de.

DOI:10.1523/JNEUROSCI.2128-08.2008

 0270-6474/08/288568-09$15.00/0

NO-GC is a heterodimer consisting of two different subunits termed α and β. Two catalytically active isoforms have been identified ($\alpha_1\beta_1$ and $\alpha_2\beta_1$) in which the β_1 subunit acts as the dimerizing partner for the α_1 or α_2 subunit (Russwurm and Koesling, 2002). Recently, mice deficient for the β_1 subunit (GC-KO mice) have been generated, which are completely devoid of NO-GC activity (Friebe et al., 2007). In the present study, we investigated the nociceptive behavior of GC-KO mice in models of acute, inflammatory, and neuropathic pain. We further characterized the distribution of NO-GC in the spinal cord and in dorsal root ganglia (DRGs), and the colocalization of NO-GC with cGKI, to further elucidate the role of cGMP in nociceptive processing.

Materials and Methods

Animals. Experiments were performed in 6- to 14-week-old mice lacking the β_1 subunit of NO-GC (GC-KO) and littermate wild-type (WT) mice of either sex backcrossed onto C57BL/6 background for >10 generations (Friebe et al., 2007). Mice were bred and maintained at the animal facility of the Institute of Pharmacology and Toxicology, University of Bochum, Germany, and were fed with fiber-free diet to avoid the second phase of mortality in GC-KO mice, which occurs because of intestinal dysmotility (Friebe et al., 2007). All experiments were approved by the local Ethics Committee for Animal Research.

Immunohistochemistry. WT ($n = 8$) and GC-KO ($n = 7$) mice were intracardially perfused with 0.9% saline followed by 4% paraformaldehyde in 0.1 M PBS, pH 7.4, under deep ketamine/xylazine anesthesia. The lumbar spinal cord and DRGs (L1–L5) were dissected and postfixed in the same fixative for 30–120 min (spinal cord) or washed several times in PBS (DRGs). After cryoprotection in 20% sucrose, tissues were frozen in tissue freezing medium on dry ice and cryostat sectioned at a thickness of 16 μm (spinal cord) or 10 μm (DRGs). Double labeling of the NO-GC β_1 subunit (GCβ_1) with calcitonin gene-related peptide (CGRP), *Griffonia simplicifolia* isolectin B4 (IB4), neurofilament 200 (NF200), myelin basic protein (MBP), glial fibrillary acidic protein (GFAP), or CD11b in the spinal cord was performed as described previously (Schmidtko et al., 2008) using rabbit anti-GCβ_1 (1:500) (Friebe et al., 2007), mouse anti-CGRP (1:500; Sigma-Aldrich), FITC-conjugated IB4 (10 μg/ml, Sigma-Aldrich), mouse anti-NF200 (clone N52, 1:1000; Sigma-Aldrich), mouse anti-MBP (1:800; Covance), mouse anti-GFAP (1:1000; Millipore), rat anti-mouse CD11b (1:300; AbD; Serotec) and species specific secondary antibodies conjugated with Alexa Fluor 488 (Invitrogen) or Cy3 (Sigma-Aldrich).

Double labeling of GCβ_1 with the neurokinin 1 receptor (NK1-R), glutamate decarboxylase 67 (GAD67) or cGKI, and of cGKI with natriuretic peptide receptor B (NPR-B) was performed using the tyramide signal amplification (TSA) technique, which allows double-label immunohistochemistry with antibodies from the same species (Shindler and Roth, 1996; Marvizon et al., 2007). Sections were permeabilized for 5 min in PBST (0.1% Triton X-100 in PBS), blocked for 30 min in blocking buffer (0.5% blocking reagent in PBS), and incubated overnight at 4°C with rabbit anti-NK1-R (1:32,000; Novus Biologicals), rabbit anti-GAD67 (1:8000; Millipore), or rabbit anti-cGKI (1:8000; recognizes the α and β isoforms of cGKI) (Pfeifer et al., 1998) dissolved in blocking buffer. Control experiments confirmed that the concentration of these antibodies was below the detection limit of the Alexa Fluor 488-labeled secondary antibody. Then sections were incubated with biotin-xx goat anti-rabbit (1:100; Invitrogen) dissolved in PBS for 1 h, followed by rabbit anti-GCβ_1 (1:500) dissolved in blocking buffer overnight or rabbit anti-NPR-B (1:100; Abgent) dissolved in blocking buffer over 3 nights, and Alexa Fluor 488 goat anti-rabbit (1:800; Invitrogen) dissolved in PBS for 2 h. Thereafter, the TSA reaction was performed by incubating sections with streptavidin-HRP (1:100) dissolved in PBS for 30 min and cyanine 3 tyramide (1:100) dissolved in amplification diluent for 2–6 min (TSA Cyanine 3 System; PerkinElmer Life and Analytical Sciences). Sections were washed three times in PBST between each step. After immunostaining, slides were immersed for 5 min in 0.06% Sudan black B (in 70% ethanol) to reduce lipofuscin-like autofluorescence (Schnell et al., 1999; Schmidtko et al., 2005), rinsed in PBS, and coverslipped in Flouromount G (Southern Biotech). Images were obtained using an Eclipse E600 microscope (Nikon) equipped with a Kappa DX 20 H camera and Kappa ImageBase software. Controls for the TSA procedure included (1) omitting the first and/or the second primary antibodies, (2) omitting the first and/or the second secondary antibodies, (3) omitting cyanine 3 tyramide, and (4) comparing the staining pattern of each antibody after TSA procedure with the staining pattern obtained in single labeling experiments using conventional immunohistochemistry on adjacent slices.

For triple labeling of GCβ_1, caveolin-1, and α-smooth muscle actin, DRG sections were incubated with rabbit anti-GCβ_1 (1:800), goat anti-caveolin-1 (1:100; Abcam) and FITC-labeled mouse anti-α-smooth muscle actin (clone 1A4; 1:500; Sigma-Aldrich) in antibody diluent (Invitrogen) overnight. Then, sections were rinsed in PBS and incubated with secondary antibodies (Alexa 647-conjugated donkey anti-rabbit IgG, 1:200; Alexa 555 donkey anti-goat IgG, 1:100) dissolved in antibody diluent. Sections were rinsed in PBS and coverslipped with Mowiol. Slides were evaluated using a Zeiss LSM 510 META confocal microscope using appropriate filters and laser combinations.

Western blot. Tissue samples from WT and GC-KO mice ($n = 3$ per group) were homogenized in buffer containing 50 mM triethanolamine, 50 mM NaCl, 1 mM EDTA, pH 7.4, 200 μM benzamidine, 1 μM pepstatin A, 500 μM PMSF, and 2 mM DTT. Western blot analyses of extracted proteins (30 μg per lane) were performed as described previously (Schmidtko et al., 2008). Blots were incubated with anti-GCβ_1 (1:1000) or anti-glyceraldehyde-3-phosphate-dehydrogenase (GAPDH; 1:2000; Ambion) for 2 h.

Behavioral testing. Littermate wild-type and GC-KO mice were used in all behavioral tests. Animals were habituated to the experimental room and were investigated by observers blinded for the genotype and treatment of the animals.

Rotarod test. Motor coordination was assessed with a Rotarod treadmill for mice (Ugo Basile) at a constant rotating speed of 32 rpm. All mice had four training sessions before the day of the experiment. The fall-off latency was averaged from six tests and the cutoff time was 120 s.

Hot-plate test. Mice were placed into a Plexiglas cylinder (diameter, 20 cm; height, 18 cm) on a metal surface maintained at 52.5°C (Hot Plate; Ugo Basile). The time between placement and shaking or licking of the hindpaws was recorded. A 30 s cutoff was used to prevent tissue damage. Only one test per animal was performed because repeated measures might cause profound latency changes (Mogil et al., 1999).

Tail-flick test. Mice were loosely wrapped in a felt towel with the tail extended. A radiant heat stimulus (Plantar test; Ugo Basile) was applied to the middle of the tail. The cutoff time was 10 s to prevent tissue injury. The tail-flick latency was calculated as the mean of three measurements with at least 5 min in between.

Dynamic-plantar test. The mechanical sensitivity of the plantar side of a hindpaw was assessed with an automated von Frey-type testing device (Dynamic Plantar Aesthesiometer; Ugo Basile). The steel rod (2 mm diameter) was pushed against the paw with ascending force until a strong and immediate withdrawal occurred. The force went from 0 to 5 g over a 10 s period and then remained constant at 5 g for an additional 10 s (cutoff time, 20 s). The paw withdrawal latency was calculated as the mean of three consecutive trials with at least 20 s in between.

Formalin test. A 5% formaldehyde solution (15 μl; formalin) was injected subcutaneously into the dorsal surface of one hindpaw (Hunskaar et al., 1985; Tjølsen et al., 1992). The time spent licking the formalin-injected paw was recorded in 5 min intervals up to 45 min after formalin injection.

Zymosan-induced mechanical hyperalgesia. The paw withdrawal latencies after mechanical stimulation were measured as described above (dynamic-plantar test). After baseline measurements, 15 μl of a zymosan A suspension (5 mg/ml in 0.1 M PBS, pH 7.4; Sigma-Aldrich) was injected into the plantar subcutaneous space of a hindpaw (Meller and Gebhart, 1997) and withdrawal latencies were determined at 2, 3, 4, 5, 6, and 8 h after zymosan injection. For determination of the zymosan-induced paw edema, mice were killed at the end of the observation period and both hindpaws were cutoff at the ankle joints. The paws were weighted and the

percentage increase in the weight of the zymosan-injected hindpaw normalized to the noninjected hindpaw of each animal was calculated.

Neuropathic pain. The "spared nerve injury" (SNI) model was used to investigate neuropathic pain. Mice were anesthetized with isoflurane, and the tibial and common peroneal branches of the sciatic nerve were ligated and sectioned distally, leaving the sural nerve intact (Decosterd and Woolf, 2000). Mechanical allodynia was determined as described above (dynamic-plantar test). Cold allodynia was measured on a 15°C cold plate (AHP-1200CPHC; Teca). The time between placement and shaking, flinching or licking the SNI-operated hindpaw was recorded. A 30 s cut-off was used. Measurements were conducted at 2 and 1 d before SNI surgery (baseline), and at 3, 7, 10, 14, 21, 28, and 35 d after SNI surgery.

Mechanical allodynia after intrathecal drug administration. The following drugs were used: 1-hydroxy-2-oxo-3-(3-aminopropyl)-3-isopropyl-1-triazene (NOC-5; Alexis Biochemicals), carbon monoxide-releasing molecule-A1 (CORM-A1) (Motterlini et al., 2005), 8-(4-chlorophenylthio)guanosine-3′,5′-cyclic monophosphate (8-pCPT-cGMP; Biolog), Rp-8-pCPT-cGMPS (Biolog), C-type natriuretic peptide (CNP; Calbiochem), and atrial natriuretic peptide (ANP; Calbiochem). For intrathecal delivery of drugs, a catheter was implanted onto the lumbosacral spinal cord (L4–L5) as described previously (Schmidtko et al., 2008). The mechanical sensitivity of both hindpaws was assessed as described above (dynamic-plantar test). After baseline measurements, drugs dissolved in 0.9% saline were intrathecally injected in a volume of 2 μl, followed by 4 μl of artificial CSF [(in mM) 141.7 Na^+, 2.6 K^+, 0.9 Mg^{2+}, 1.3 Ca^{2+}, 122.7 Cl^-, 21.0 HCO_3^-, 2.5 HPO_4^{2-}, and 3.5 dextrose, bubbled with 5% CO_2 in 95% O_2 to adjust pH to 7.2]. In coadministration experiments, Rp-8-pCPT-cGMPS was injected 1 min before NOC-5 or CNP. After drug injection, the paw withdrawal latencies were determined in intervals of 15 or 30 min. After the experiment, mice were killed and the catheter position was verified by injection of 5 μl of methylene blue. Only animals in which methylene blue marked the lumbar spinal cord were included.

Statistics. Statistical evaluation was done with SPSS 12.0.1 for Windows (Microsoft). The Kolmogorov–Smirnov test was used to assess normal distribution of data within groups. Normally distributed data were analyzed with Student's *t* test or repeated measures of ANOVA followed by Fisher's *post hoc* test and are presented as the mean ± SEM. Rotarod fall-off latencies were analyzed with Mann–Whitney *U* test and are expressed as median and interquartile range. For all tests, $p < 0.05$ was considered as statistically significant.

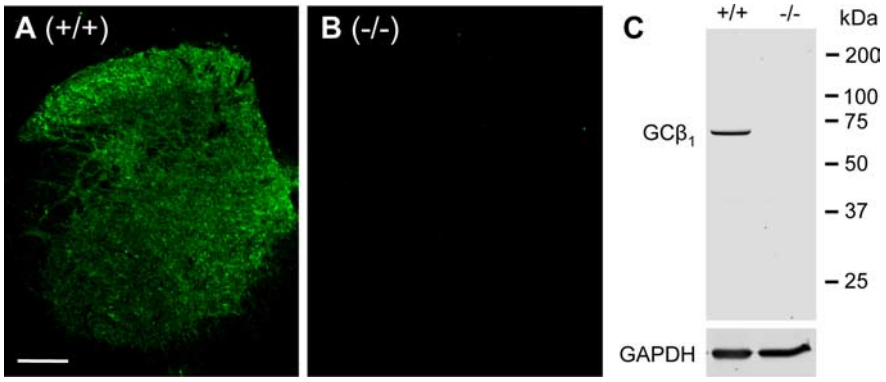

Figure 1. Expression of NO-GC in the spinal cord. ***A***, ***B***, Immunohistochemistry of the GCβ1 subunit of NO-GC in the lumbar spinal cord in wild-type mice (***A***) and in GC-KO mice (***B***) reveals specific NO-GC expression throughout the spinal cord with strong immunoreactivity in the dorsal horn and around the central canal. Scale bar, 100 μm. ***C***, Western blot of GCβ1 (70 kDa) with spinal cord homogenates of wild-type mice (left) and GC-KO mice (right) confirms the specificity of the antibody. GAPDH (36 kDa) was used as loading control.

Results

NO-GC expression in the spinal cord and in dorsal root ganglia

NO-GC expression in the spinal cord

Immunohistochemical studies of the mouse spinal cord revealed immunoreactivity of GCβ_1 throughout the gray matter with the most intense staining in the dorsal horn and around the central canal (Fig. 1*A*). Specificity of anti-GCβ_1 was confirmed by the absence of immunoreactivity in the spinal cord of GC-KO mice (Fig. 1*B*) and by Western blot analyses detecting a single band at the estimated molecular weight of 70 kDa in spinal cord protein extracts of wild-type mice, but not in extracts derived from GC-KO mice (Fig. 1*C*).

The detailed distribution of GCβ_1 in the dorsal horn of the spinal cord was investigated by double-labeling immunohistochemistry experiments with established markers. GCβ_1 immunoreactivity was detected in lamina I projection neurons expressing NK1-R (Fig. 2*A–D*) and in GABAergic interneurons in lamina II and III expressing GAD67 (Fig. 2*E–H*). GCβ_1 did not colocalize with CGRP-positive (Fig. 2*I–L*) and IB4-binding (Fig. 2*M–P*) terminals of nociceptive primary afferents in lamina I and II. Furthermore, no colocalization was detected between GCβ_1 and markers of large, myelinated primary afferents (neurofilament 200, clone N52), oligodendrocytes (myelin basic protein), astrocytes (glial fibrillary acidic protein), or microglia (CD11b) (supplemental Fig. 1, available at www.jneurosci.org as supplemental material). These data show that in the dorsal horn of the mouse spinal cord, GCβ_1 is expressed in projection neurons in lamina I and in inhibitory interneurons of lamina II and III.

NO-GC expression in DRGs

In DRGs, immunoreactivity for GCβ_1 was confined to non-neuronal cells. It was present in a subset of satellite cells identified by their typical perineuronal localization and morphology (Fig. 3*A*,*B*), in α-smooth muscle actin negative pericytes that ensheath caveolin-1-immunoreactive capillary endothelial cells (Fig. 3*A*,*B*,*E*) and in smooth muscle cells of blood vessels identified by their morphology and immunoreactivity for α-smooth muscle actin (Fig. 3*A*,*B*,*F*). No GCβ_1 immunoreactivity was detected in DRGs of GC-KO mice (Fig. 3*C*,*D*).

Acute, inflammatory, and neuropathic pain behavior in GC-KO mice

To assess the role of NO-GC in nociceptive processing *in vivo*, we compared the nociceptive behavior of GC-KO mice with that of littermate WT mice in models of acute, inflammatory, and neuropathic pain. The mean body weight of GC-KO and WT mice was 17.1 ± 0.5 g and 20.6 ± 0.8 g, respectively. The macroscopic morphology of the spinal cord and the distribution of terminals of nociceptive and thermoreceptive primary afferents in the superficial dorsal horn appeared normal in GC-KO mice (data not shown). The motor coordination and balance was not impaired in GC-KO mice, as analyzed in the rotarod test (median fall-off latencies: GC-KO mice, 107.2 s; interquartile range, 93.1–113.8 s; $n = 6$; WT mice, 101.0 s; interquartile range, 73.5–117.2 s; $n = 8$; $p = 0.795$). Similarly, no motor impairments in GC-KO mice were observed in the vertical pole test and in the hanging wire test (data not shown).

To determine whether or not acute nociception is altered in GC-KO mice, the latency to acute thermal and mechanical stimuli was measured using the hot-plate test (52.5°C), the tail-flick test, and a von Frey-like test that analyses paw withdrawal laten-

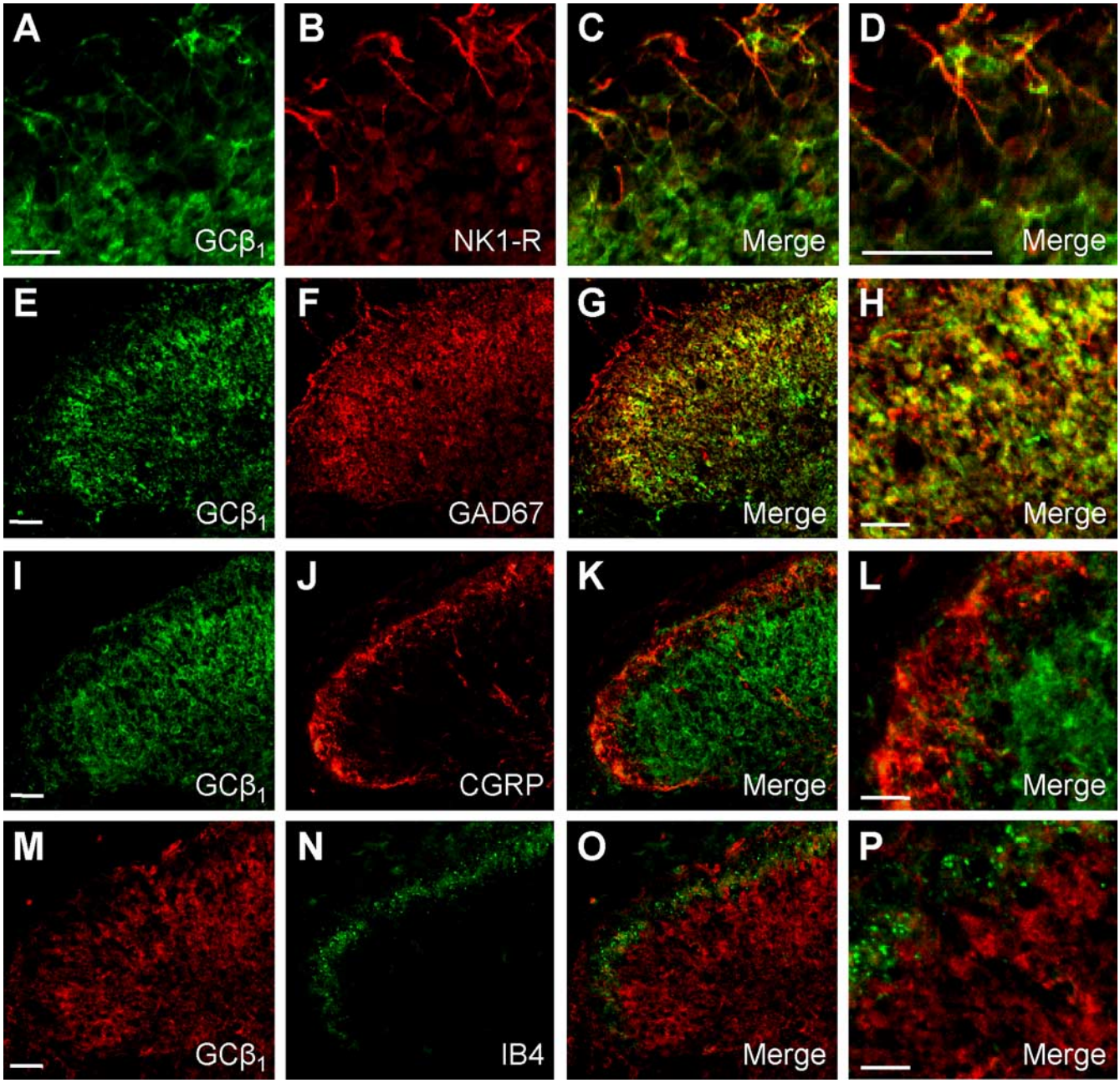

Figure 2. Double labeling of NO-GC with markers in the dorsal horn of the spinal cord. ***A***, ***E***, ***I***, ***M***, GCβ1 immunoreactivity. ***B***, ***F***, ***J***, ***N***, Immunoreactivity for NK1-R, GAD67, CGRP, and IB4. ***C***, ***G***, ***K***, ***O***, Merged images with colocalization indicated in yellow. ***D***, ***H***, ***L***, ***P***, Merged images at higher magnification. The experiments revealed that NO-GC colocalizes with NK1-R and GAD67, but not with CGRP or IB4. Scale bars: ***A***, ***D***, ***H***, ***L***, ***P***, 25 μm; ***E***, ***I***, ***M***, 50 μm.

cies after automated mechanical stimulation (dynamic-plantar test). In these tests of acute nociception, no significant differences in latency times were found between GC-KO and WT mice (Table 1). These data indicate that the immediate response to acute noxious thermal and mechanical stimulation is intact in GC-KO mice.

We then analyzed the responses of GC-KO mice in models of inflammatory pain. In the formalin test, a nociceptive response consisting of licking the formalin-injected hindpaw was observed in both groups. In the first phase (1–10 min), which results from direct activation of primary afferent nociceptors, the licking behavior of GC-KO and WT mice was similar (Fig. 4*A*,*B*) ($p = 0.559$). However, the second phase of paw licking that involves a period of sensitization was dramatically reduced in GC-KO mice compared with WT mice (Fig. 4*A*,*B*) ($p = 0.004$), suggesting an important contribution of NO-GC to the formalin-induced rapid sensitization in pain pathways. In a second model of inflammatory pain, the mechanical hyperalgesia was monitored after injection of zymosan into a hindpaw (Fig. 4*C*). During the first 4 h after zymosan injection, mechanical hyperalgesia developed similarly in both groups. However, at later time points (i.e., between 5 h after zymosan injection and the end of the 8 h observation period), the extent of mechanical hyperalgesia was significantly reduced in GC-KO mice compared with WT mice (Fig. 4*C*). This reduced paw sensitivity was not associated with any significant difference in zymosan-evoked paw edema, which was analyzed 8 h after zymosan injection. The percentage increase in the weight of the zymosan-injected hindpaw compared with the

noninjected hindpaw was 42.6 ± 9.0% and 35.4 ± 6.5% in GC-KO and WT mice, respectively ($p = 0.517$). Together, the data suggest an essential contribution of NO-GC to exaggerated pain sensitivity during inflammatory pain.

The role of NO-GC in neuropathic pain was tested in the SNI model (Decosterd and Woolf, 2000) by analyzing SNI-induced mechanical and cold allodynia. During the first 7 d after nerve injury, mechanical allodynia of the affected hindpaw developed similarly in GC-KO and WT mice (Fig. 4*D*). However, at later stages, GC-KO mice gradually recovered from mechanical allodynia reaching paw withdrawal latency times comparable with those before SNI surgery, whereas in WT mice mechanical allodynia remained nearly constant until the end of the 35 d observation period (Fig. 4*D*). The SNI surgery also produced cold allodynia in both GC-KO and WT mice (Fig. 4*E*). Similar to the mechanical allodynia, the extent of cold allodynia did not differ between both groups during the first days after injury, but from 10 to 35 d after injury the cold allodynia was significantly reduced in GC-KO mice compared with WT mice (Fig. 4*E*). These data suggest that NO-GC plays an important role in the maintenance of neuropathic pain after peripheral traumatic axonal injury, but it seems not to be critically involved in the induction of neuropathic pain during the first days after injury.

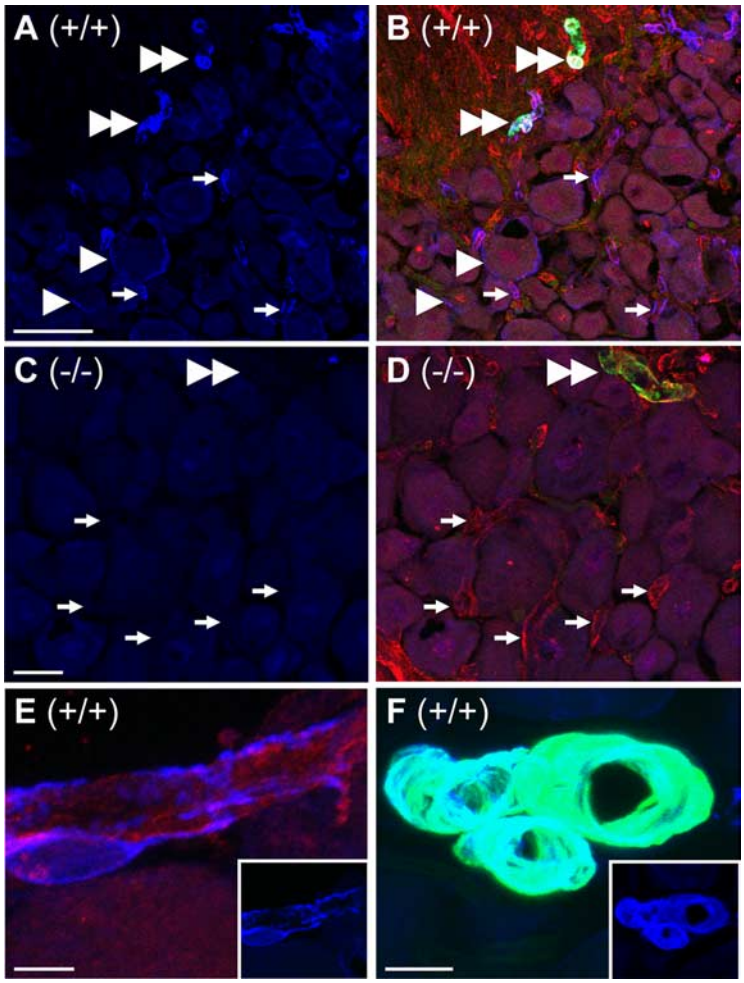

Figure 3. Expression of NO-GC in DRGs. Triple labeling of GCβ1 (blue), caveolin-1 (red), and α-smooth muscle actin (green) demonstrates that NO-GC is expressed in satellite cells, in pericytes around capillary endothelial cells, and in smooth muscle cells, but not in DRG neurons. ***A***, ***B***, Wild-type mouse. ***C***, ***D***, GC-KO mouse. Arrows, Pericytes around capillary endothelial cells; arrowheads, satellite cells; doubled arrowheads, blood vessels. ***E***, GCβ1-immunoreactive pericyte. Inset, Same area as in ***E***, but GCβ1-immunoreactivity only is shown. ***F***, GCβ1-immunoreactive small blood vessels. Inset, Same area as in ***F***, but GCβ1-immunoreactivity only is shown. Scale bars: (in ***A***) ***A***, ***B***, 50 μm; (in ***C***) ***C***, ***D***, 20 μm; ***E***, 5 μm; ***F***, 10 μm.

Table 1. Acute nociception in GC-KO mice

Model	GC-KO mice	WT mice	*p*	*n* (per group)
Hot-plate test (52.5°C)	20.0 ± 1.3 s	15.6 ± 2.0 s	0.122	8
Tail-flick test	6.6 ± 0.3 s	7.0 ± 0.2 s	0.285	6
Dynamic-plantar test	7.5 ± 0.6 s	7.4 ± 0.7 s	0.937	8

NO-, CO-, and cGMP-induced pain behavior in GC-KO mice

To assess the impact of NO-GC for NO, CO, and cGMP signaling in spinal nociceptive processing, we determined the nociceptive behavior of GC-KO and WT mice after intrathecal administration of the NO donor NOC-5, the CO-releasing molecule CORM-A1 (Motterlini et al., 2005), or the cGMP analog 8-pCPT-cGMP. Injection of NOC-5 (50 nmol, i.t.) evoked mechanical allodynia in WT mice, which was completely absent in GC-KO mice (Fig. 5*A*). Interestingly, administration of CORM-A1 (40 nmol, i.t.) also produced mechanical allodynia in WT mice but not in GC-KO mice (Fig. 5*B*). Mechanical allodynia was not observed after administration of the inactive form of CORM-A1 (iCORM-A1; 40 nmol, i.t.), which was used as negative control to exclude the possibility of nonspecific effects (data not shown). In contrast to NOC-5 and CORM-A1, administration of 8-pCPT-cGMP (15 nmol, i.t.) evoked mechanical allodynia in both GC-KO and WT mice to a similar extent (Fig. 5*C*). These data show that NO-GC is indispensable for the pronociceptive effects of i.t. administered NO and CO-releasing compounds, and that cGMP-dependent pronociceptive signaling pathways, as expected, are intact in GC-KO mice.

Signaling between NO-GC and cGKI

It has been speculated in several reports that the pronociceptive effects of the NO/cGMP signaling pathway are mediated by activation of cGKI (Qian et al., 1996; Tao et al., 2000; Tegeder et al., 2004; Song et al., 2006; Sung et al., 2006). To assess the impact of cGKI as a downstream effector of NO-dependent cGMP production in DRGs and the spinal cord, double-labeling immunohistochemistry experiments of GCβ_1 and cGKI were performed. Interestingly, in DRGs, no colocalization of GCβ_1 with cGKI was detected (Fig. 6*A–C*). In the spinal cord, GCβ_1 was colocalized with cGKI in some neurons of lamina I and III. However, many of the GCβ_1-positive neurons did not express cGKI, as did many cGKI-positive neurons not express GCβ_1 (Fig. 6*D–F*). We concluded that cGMP produced by natriuretic peptide-activated

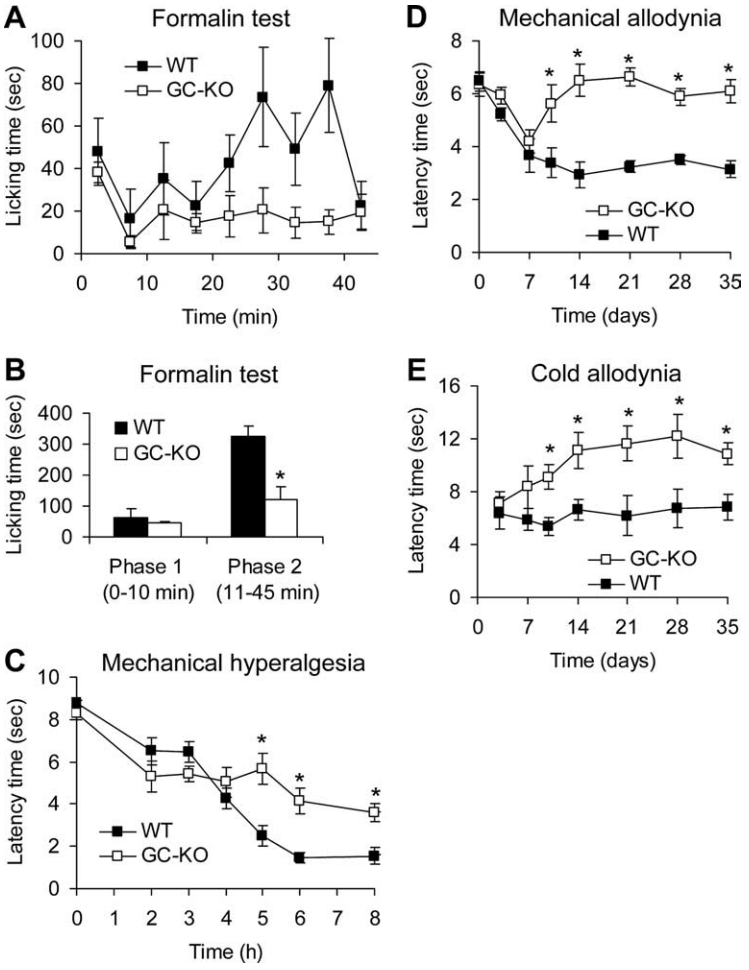

Figure 4. Inflammatory and neuropathic pain in GC-KO mice. ***A***, ***B***, Formalin test. ***A***, Time course of licking behavior of the formalin-injected hindpaw. ***B***, Sum of paw-licking time in phase 1 (0–10 min) and phase 2 (11–45 min). Note that the licking behavior in phase 2 is considerably reduced in GC-KO mice. ***C***, Zymosan-induced mechanical hyperalgesia. Time course of paw withdrawal latency time after mechanical stimulation demonstrates reduced mechanical hyperalgesia in GC-KO mice at time points ≥5 h. ***D***, ***E***, SNI-induced neuropathic pain in GC-KO mice. ***D***, Mechanical allodynia. Time course of paw withdrawal latency time after mechanical stimulation. ***E***, Cold allodynia. Time course of latency time to shake, flinch, or lick the SNI-operated hindpaw after placement on a 15°C cold plate. Before SNI surgery, all animals stayed on the cold plate for 30 s (cutoff) without paw shaking, flinching, or licking. Data indicate that the maintenance of neuropathic pain (at time points ≥10 d), but not the induction of neuropathic pain, is impaired in GC-KO mice. All data are presented as mean ± SEM. $*p < 0.05$, comparing GC-KO and WT mice; $n = 6–8$ (GC-KO) or 8 (WT) per group.

guanylyl cyclases might contribute to cGKI activation during nociceptive processing. Indeed, NPR-B showed an almost identical staining pattern in DRG neurons compared with cGKI (Fig. 6*G–I*). No specific staining of NPR-B was detected in the spinal cord.

We then analyzed the functional impact of NO-GC and natriuretic peptide-activated guanylyl cyclases for cGKI activation during nociceptive processing. For this purpose, the NO donor NOC-5, the NPR-A ligand ANP, or the NPR-B ligand CNP were intrathecally injected in mice with or without pretreatment of the cGKI inhibitor Rp-8-pCPT-cGMPS, and the nociceptive behavior was determined. Of note, in line with the different staining pattern of GCβ_1 and cGKI described above, the mechanical allodynia evoked by NOC-5 (50 nmol, i.t.) was not prevented by pretreatment with Rp-8-pCPT-cGMPS (10 nmol, i.t.) (Fig. 7*A*). In contrast, administration of the NPR-B ligand CNP (200 ng, i.t.) evoked mechanical allodynia that was antagonized by pretreatment with Rp-8-pCPT-cGMPS (Fig. 7*B*). Mechanical allodynia did not occur after injection of the NPR-A ligand ANP (200 ng, i.t.) (Fig. 7*B*). Collectively, these data indicate that during nociceptive processing cGMP produced by NO-GC obviously stimulates targets different from cGKI, and that cGMP produced by NPR-B may contribute to nociceptive signaling by activation of cGKI.

Discussion

In the present study, we show that NO-GC essentially contributes to the sensitization of pain pathways. NO-GC is expressed in lamina I projection neurons and in inhibitory interneurons in the dorsal horn of the mouse spinal cord, whereas in dorsal root ganglia its distribution is restricted to non-neuronal cells. Mice lacking NO-GC exhibit a considerably attenuated nociceptive behavior in models of inflammatory and neuropathic pain, whereas their responses are normal in models of acute pain. In addition we show that cGMP produced by NO-GC unexpectedly activates pain signaling pathways different from cGKI.

The distribution of NO-GC in the spinal cord and DRGs has been investigated in previous studies using antibodies from different sources with, however, contradictory results (Maihöfner et al., 2000; Tao and Johns, 2002; Ding and Weinberg, 2006; Ruscheweyh et al., 2006). Using an anti-GCβ_1 antibody (Friebe et al., 2007) whose specificity was confirmed by immunohistochemical and Western blot analyses in tissue of GC-KO mice, we here demonstrate that NO-GC is expressed in NK1-R-positive projection neurons and in GAD67-positive inhibitory interneurons, whereas it is absent in central terminals of primary afferent neurons and in glial cells of the mouse spinal cord. This staining pattern is similar to the distribution of NO-GC in the spinal cord of rats that was reported recently by Ruscheweyh et al. (2006) and Ding (2006). In DRGs, we found NO-GC to be expressed in satellite cells, pericytes, and smooth muscle cells of blood vessels, but unexpectedly not in neurons. In contrast, Ruscheweyh et al. (2006) detected GCβ_1 immunoreactivity in 12% of lumbar DRG neurons. To clarify this discrepancy, we tested the antibody used in the cited study (Cayman 160897) and observed similar GCβ_1 immunoreactivity in DRG neurons of wild-type and GC-KO mice (data not shown). Thus, we conclude that the immunoreactivity detected in DRG neurons (Ruscheweyh et al., 2006) was caused by unspecific binding and that the distribution of NO-GC in DRGs is indeed restricted to non-neuronal cells. This conclusion is supported by previous studies that demonstrated that incubation of DRG sections with an NO donor or axotomy of the sciatic nerve caused an increase of cGMP levels selectively in satellite cells but not in DRG neurons (Morris et al., 1992; Shi et al., 1998).

The presence of NO-GC in projecting neurons and inhibitory interneurons of the spinal cord, as well as in satellite cells of DRGs, is consistent with an important contribution of NO-GC to

nociceptive processing. The pivotal role of NK1-R-positive lamina I projection neurons in this context has been demonstrated by many approaches. Selective ablation of these neurons attenuated hyperalgesia and allodynia in models of inflammatory and neuropathic pain (Mantyh et al., 1997; Nichols et al., 1999; Khasabov et al., 2002). Moreover, injection of formalin or capsaicin into a hindpaw induced LTP of synaptic strength at synapses between C-fibers and lamina I neurons projecting to the periaqueductal gray. This form of LTP is NO-dependent because it can be prevented by an NOS inhibitor (Ikeda et al., 2006). The importance of inhibitory dorsal horn neurons for nociceptive processing is reflected by observations such that blocking GABA-mediated inhibition produces a pattern of pain hypersensitivity very similar to that of neuropathic pain (Sivilotti and Woolf, 1994), and that a functional loss of GABAergic inhibition in the spinal cord contributes to the allodynia after peripheral nerve injury (Moore et al., 2002). There is accumulating evidence that satellite cells in DRGs are also implicated in nociceptive processing (Scholz and Woolf, 2007). In response to P2X7 receptor activation by ATP, satellite cells release tumor necrosis factor α, which in turn increases the excitability of DRG neurons. Of note, P2X7 receptors are expressed only in satellite cells in DRGs and P2X7 knock-out mice do not develop neuropathic pain after nerve ligation (Zhang et al., 2007). Furthermore, the MAP (mitogen-activated protein) kinases ERK (extracellular signal-regulated kinase) and p38 are activated and the expression of metalloprotease 2 is induced in satellite cells after peripheral nerve injury (Zhuang et al., 2005; Kawasaki et al., 2008). Thus, the distribution pattern of NO-GC in both dorsal horn neurons and DRG satellite cells indicates that it might modulate nociceptive processing at different sites.

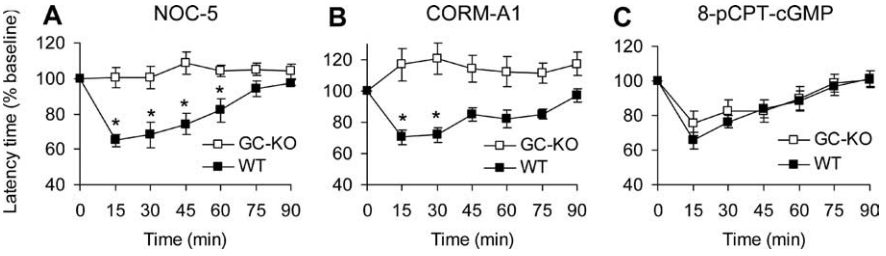

Figure 5. NO-, CO-, and cGMP-induced nociceptive behavior in GC-KO mice. ***A–C***, Time course of mechanical allodynia induced by intrathecal administration of NOC-5 (NO donor, 50 nmol; ***A***), CORM-A1 (CO-releasing molecule, 40 nmol; ***B***), or 8-pCPT-cGMP (cGMP analog, 15 nmol; ***C***). No allodynia was observed in GC-KO mice after administration of NOC-5 or CORM-A1, whereas 8-pCPT-cGMP-induced allodynia was intact. The hindpaw withdrawal latency times after mechanical stimulation were normalized to baseline latency times and are presented as mean percentage ± SEM. *$p < 0.05$, comparing GC-KO and WT mice; $n = 6$ per group.

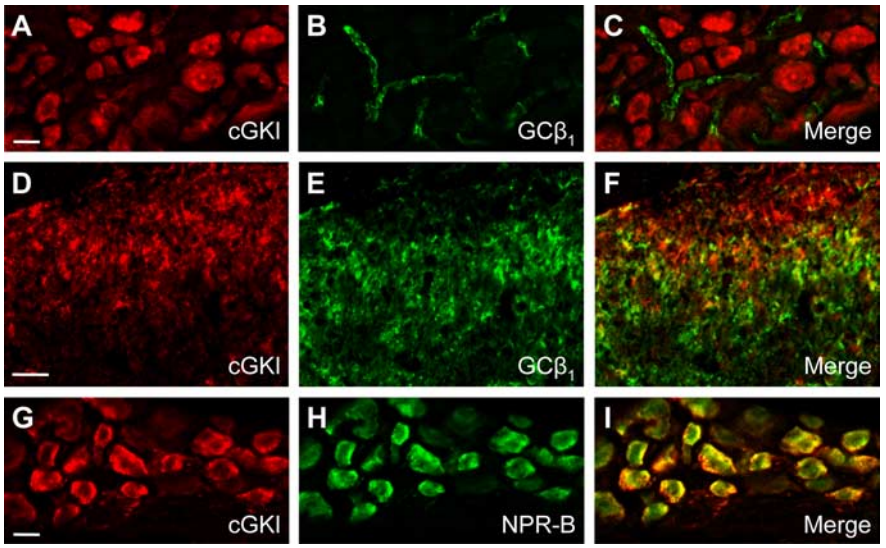

Figure 6. Double labeling of cGKI with NO-GC and NPR-B in DRGs and in the dorsal horn of the spinal cord. ***A***, ***D***, ***G***, cGKI immunoreactivity, ***B***, ***E***, ***H***, Immunoreactivity for GCβ1 or NPR-B. ***C***, ***F***, ***I***, Merged images with colocalization being indicated in yellow. The experiments revealed that cGKI and NO-GC are not colocalized in DRGs and only partially colocalized in the spinal cord, whereas cGKI colocalizes with NPR-B in DRGs. Scale bars, 25 μm.

Acute nociceptive responses were unaffected in GC-KO mice as observed in the hot-plate test, the tail-flick test, after mechanical stimulation of a naive hindpaw, and in the immediate response to formalin injection (phase 1). However, GC-KO mice demonstrated a considerably reduced nociceptive behavior in inflammatory and neuropathic pain models, i.e., in the second phase of the formalin test, and in late stages of the zymosan-induced mechanical hyperalgesia (≥5 h) and the SNI-induced mechanical or cold allodynia (≥10 d). Moreover, we show that NO-GC is essential for the pronociceptive actions of both NO and CO, because GC-KO mice, in contrast to WT mice, failed to develop mechanical allodynia after intrathecal injection of the NO donor NOC-5 or the CO-releasing molecule CORM-A1. These data suggest that NO- and CO-mediated cGMP synthesis is not involved in acute pain reflexes, but it plays a pivotal role in the mechanisms underlying exaggerated sensitivity in inflammatory and neuropathic pain. The data further confirm the antinociceptive effects of the NO-GC inhibitor ODQ (1*H*-[1,2,4]oxadiazolo-[4,3-a]quinoxalin-1-one) in models of inflammatory or neuropathic pain (Ferreira et al., 1999; Kawamata and Omote, 1999; Tao and Johns, 2002; Song et al., 2006).

Our observation that NO-GC only partially colocalizes with cGKI was quite surprising. In fact, a functional NO/NO-GC/cGMP/cGKI pathway is present in many other brain regions and it contributes, for example, to LTP in the hippocampus (Zhuo et al., 1994). In previous studies, we and others demonstrated that cGKI is expressed in many DRG neurons and in the superficial dorsal horn of the spinal cord, and that intrathecal administration of cGKI inhibitors or genetic knock-out of cGKI reduces the nociceptive behavior in models of inflammatory pain (Qian et al., 1996; Tao et al., 2000; Schmidtko et al., 2003; Tegeder et al., 2004). Therefore, one might have speculated that cGMP produced by NO-GC exerts its pronociceptive effects by activation of cGKI. However, we here demonstrate that NO-GC and cGKI are colocalized only in some neurons in laminas I and III of the spinal cord, but not in DRGs. This implies (1) that at least some of the "pain-relevant" effects of NO-GC might be mediated by targets different from cGKI, and (2) that upstream effectors different from NO-GC may provide cGMP for cGKI activation during nociceptive processing. Possible candidates are the "particulate"

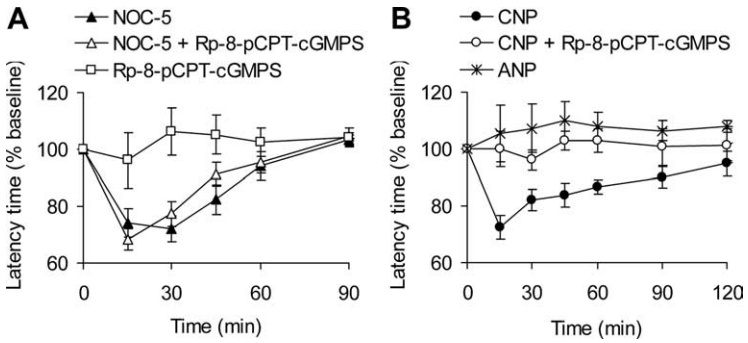

Figure 7. Effect of cGKI inhibition on the nociceptive behavior induced by activators of NO-GC and natriuretic peptide-activated GCs. ***A***, ***B***, Time course of mechanical allodynia induced by intrathecal administration of NOC-5 (NO donor, 50 nmol), Rp-8-pCPT-cGMPS (cGKI inhibitor, 10 nmol), or the combination of NOC-5 (50 nmol) and Rp-8-pCPT-cGMPS (10 nmol) (***A***), and CNP (NPR-B activator, 200 ng), ANP (NPR-A activator, 200 ng), or the combination of CNP (200 ng) and Rp-8-pCPT-cGMPS (10 nmol) (***B***). Data indicate that the cGKI inhibitor antagonizes CNP-induced allodynia but not NOC-5-induced allodynia. The hindpaw withdrawal latency times after mechanical stimulation were measured at the indicated time points. Data were normalized to baseline latency times and are presented as mean percentage ± SEM; $n = 6$ or 8 per group.

guanylyl cyclases, of which seven forms activated by different ligands have been described in rodents (for review, see Garbers et al., 2006). We here demonstrate that the particulate guanylyl cyclase NPR-B interacts with cGKI during nociceptive processing, because NPR-B and cGKI are colocalized in DRGs and the cGKI inhibitor Rp-8-pCPT-cGMPS antagonized the pronociceptive effects of the NPR-B ligand CNP but not that of the NO donor NOC-5. Interestingly, recent data indicate that during embryonic development the neuronal connectivity in the spinal cord depends on cGKI and on cGMP produced by NPR-B, but not by NO-GC (Schmidt et al., 2007). Thus, the NPR-B/cGMP/cGKI signaling pathway may have important functions in both embryonic development and nociceptive processing.

In conclusion, the distribution pattern of NO-GC in the spinal cord and DRGs, as well as the strongly inhibited nociceptive behavior of GC-KO mice, show that NO-GC-mediated cGMP production has a dominant role in the development of exaggerated pain sensitivity during inflammatory and neuropathic pain. However, the hypothesis that the pronociceptive effects of cGMP, in turn, are solely mediated by cGKI activation has to be abandoned. It remains to be determined which targets mediate the pronociceptive effects of NO-dependent cGMP production.

References

Boettger MK, Uceyler N, Zelenka M, Schmitt A, Reif A, Chen Y, Sommer C (2007) Differences in inflammatory pain in nNOS-, iNOS- and eNOS-deficient mice. Eur J Pain 11:810–818.

Chu YC, Guan Y, Skinner J, Raja SN, Johns RA, Tao YX (2005) Effect of genetic knock-out or pharmacologic inhibition of neuronal nitric oxide synthase on complete Freund's adjuvant-induced persistent pain. Pain 119:113–123.

Davis KL, Martin E, Turko IV, Murad F (2001) Novel effects of nitric oxide. Annu Rev Pharmacol Toxicol 41:203–236.

Decosterd I, Woolf CJ (2000) Spared nerve injury: an animal model of persistent peripheral neuropathic pain. Pain 87:149–158.

Ding JD, Weinberg RJ (2006) Localization of soluble guanylyl cyclase in the superficial dorsal horn. J Comp Neurol 495:668–678.

Ferreira J, Santos AR, Calixto JB (1999) The role of systemic, spinal and supraspinal L-arginine-nitric oxide-cGMP pathway in thermal hyperalgesia caused by intrathecal injection of glutamate in mice. Neuropharmacology 38:835–842.

Friebe A, Mergia E, Dangel O, Lange A, Koesling D (2007) Fatal gastrointestinal obstruction and hypertension in mice lacking nitric oxide-sensitive guanylyl cyclase. Proc Natl Acad Sci U S A 104:7699–7704.

Garbers DL, Chrisman TD, Wiegn P, Katafuchi T, Albanesi JP, Bielinski V, Barylko B, Redfield MM, Burnett JC Jr (2006) Membrane guanylyl cyclase receptors: an update. Trends Endocrinol Metab 17:251–258.

Garry MG, Richardson JD, Hargreaves KM (1994) Sodium nitroprusside evokes the release of immunoreactive calcitonin gene-related peptide and substance P from dorsal horn slices via nitric oxide-dependent and nitric oxide-independent mechanisms. J Neurosci 14:4329–4337.

Hunskaar S, Fasmer OB, Hole K (1985) Formalin test in mice, a useful technique for evaluating mild analgesics. J Neurosci Methods 14:69–76.

Ikeda H, Stark J, Fischer H, Wagner M, Drdla R, Jäger T, Sandkühler J (2006) Synaptic amplifier of inflammatory pain in the spinal dorsal horn. Science 312:1659–1662.

Kawamata T, Omote K (1999) Activation of spinal N-methyl-D-aspartate receptors stimulates a nitric oxide/cyclic guanosine 3,5-monophosphate/glutamate release cascade in nociceptive signaling. Anesthesiology 91:1415–1424.

Kawasaki Y, Xu ZZ, Wang X, Park JY, Zhuang ZY, Tan PH, Gao YJ, Roy K, Corfas G, Lo EH, Ji RR (2008) Distinct roles of matrix metalloproteases in the early- and late-phase development of neuropathic pain. Nat Med 14:331–336.

Khasabov SG, Rogers SD, Ghilardi JR, Peters CM, Mantyh PW, Simone DA (2002) Spinal neurons that possess the substance P receptor are required for the development of central sensitization. J Neurosci 22:9086–9098.

Mabuchi T, Matsumura S, Okuda-Ashitaka E, Kitano T, Kojima H, Nagano T, Minami T, Ito S (2003) Attenuation of neuropathic pain by the nociceptin/orphanin FQ antagonist JTC-801 is mediated by inhibition of nitric oxide production. Eur J Neurosci 17:1384–1392.

Maihöfner C, Euchenhofer C, Tegeder I, Beck KF, Pfeilschifter J, Geisslinger G (2000) Regulation and immunhistochemical localization of nitric oxide synthases and soluble guanylyl cyclase in mouse spinal cord following nociceptive stimulation. Neurosci Lett 290:71–75.

Malmberg AB, Yaksh TL (1993) Spinal nitric oxide synthesis inhibition blocks NMDA-induced thermal hyperalgesia and produces antinociception in the formalin test in rats. Pain 54:291–300.

Mantyh PW, Rogers SD, Honore P, Allen BJ, Ghilardi JR, Li J, Daughters RS, Lappi DA, Wiley RG, Simone DA (1997) Inhibition of hyperalgesia by ablation of lamina I spinal neurons expressing the substance P receptor. Science 278:275–279.

Marvizón JC, Pérez OA, Song B, Chen W, Bunnett NW, Grady EF, Todd AJ (2007) Calcitonin receptor-like receptor and receptor activity modifying protein 1 in the rat dorsal horn: localization in glutamatergic presynaptic terminals containing opioids and adrenergic alpha2C receptors. Neuroscience 148:250–265.

Meller ST, Gebhart GF (1993) Nitric oxide (NO) and nociceptive processing in the spinal cord. Pain 52:127–136.

Meller ST, Gebhart GF (1997) Intraplantar zymosan as a reliable, quantifiable model of thermal and mechanical hyperalgesia in the rat. Eur J Pain 1:43–52.

Meller ST, Cummings CP, Traub RJ, Gebhart GF (1994) The role of nitric oxide in the development and maintenance of the hyperalgesia produced by intraplantar injection of carrageenan in the rat. Neuroscience 60:367–374.

Mogil JS, Wilson SG, Bon K, Lee SE, Chung K, Raber P, Pieper JO, Hain HS, Belknap JK, Hubert L, Elmer GI, Chung JM, Devor M (1999) Heritability of nociception I: responses of 11 inbred mouse strains on 12 measures of nociception. Pain 80:67–82.

Moore KA, Kohno T, Karchewski LA, Scholz J, Baba H, Woolf CJ (2002) Partial peripheral nerve injury promotes a selective loss of GABAergic inhibition in the superficial dorsal horn of the spinal cord. J Neurosci 22:6724–6731.

Morris R, Southam E, Braid DJ, Garthwaite J (1992) Nitric oxide may act as a messenger between dorsal root ganglion neurones and their satellite cells. Neurosci Lett 137:29–32.

Motterlini R, Sawle P, Hammad J, Bains S, Alberto R, Foresti R, Green CJ

(2005) CORM-A1: a new pharmacologically active carbon monoxide-releasing molecule. FASEB J 19:284–286.

Nichols ML, Allen BJ, Rogers SD, Ghilardi JR, Honore P, Luger NM, Finke MP, Li J, Lappi DA, Simone DA, Mantyh PW (1999) Transmission of chronic nociception by spinal neurons expressing the substance P receptor. Science 286:1558–1561.

Pfeifer A, Klatt P, Massberg S, Ny L, Sausbier M, Hirneiss C, Wang GX, Korth M, Aszódi A, Andersson KE, Krombach F, Mayerhofer A, Ruth P, Fässler R, Hofmann F (1998) Defective smooth muscle regulation in cGMP kinase I-deficient mice. EMBO J 17:3045–3051.

Qian Y, Chao DS, Santillano DR, Cornwell TL, Nairn AC, Greengard P, Lincoln TM, Bredt DS (1996) cGMP-dependent protein kinase in dorsal root ganglion: relationship with nitric oxide synthase and nociceptive neurons. J Neurosci 16:3130–3138.

Ruscheweyh R, Goralczyk A, Wunderbaldinger G, Schober A, Sandkühler J (2006) Possible sources and sites of action of the nitric oxide involved in synaptic plasticity at spinal lamina I projection neurons. Neuroscience 141:977–988.

Russwurm M, Koesling D (2002) Isoforms of NO-sensitive guanylyl cyclase. Mol Cell Biochem 230:159–164.

Schmidt H, Stonkute A, Jüttner R, Schäffer S, Buttgereit J, Feil R, Hofmann F, Rathjen FG (2007) The receptor guanylyl cyclase Npr2 is essential for sensory axon bifurcation within the spinal cord. J Cell Biol 179:331–340.

Schmidtko A, Ruth P, Geisslinger G, Tegeder I (2003) Inhibition of cyclic guanosine 5′-monophosphate-dependent protein kinase I (PKG-I) in lumbar spinal cord reduces formalin-induced hyperalgesia and PKG upregulation. Nitric Oxide 8:89–94.

Schmidtko A, Del Turco D, Coste O, Ehnert C, Niederberger E, Ruth P, Deller T, Geisslinger G, Tegeder I (2005) Essential role of the synaptic vesicle protein synapsin II in formalin-induced hyperalgesia and glutamate release in the spinal cord. Pain 115:171–181.

Schmidtko A, Gao W, Sausbier M, Rauhmeier I, Sausbier U, Niederberger E, Scholich K, Huber A, Neuhuber W, Allescher HD, Hofmann F, Tegeder I, Ruth P, Geisslinger G (2008) Cysteine-rich protein 2, a novel downstream effector of cGMP/cGMP-dependent protein kinase I-mediated persistent inflammatory pain. J Neurosci 28:1320–1330.

Schnell SA, Staines WA, Wessendorf MW (1999) Reduction of lipofuscin-like autofluorescence in fluorescently labeled tissue. J Histochem Cytochem 47:719–730.

Scholz J, Woolf CJ (2002) Can we conquer pain? Nat Neurosci 5 [Suppl]:1062–1067.

Scholz J, Woolf CJ (2007) The neuropathic pain triad: neurons, immune cells and glia. Nat Neurosci 10:1361–1368.

Shi TJ, Holmberg K, Xu ZQ, Steinbusch H, de Vente J, Hökfelt T (1998) Effect of peripheral nerve injury on cGMP and nitric oxide synthase levels in rat dorsal root ganglia: time course and coexistence. Pain 78:171–180.

Shindler KS, Roth KA (1996) Double immunofluorescent staining using two unconjugated primary antisera raised in the same species. J Histochem Cytochem 44:1331–1335.

Sivilotti L, Woolf CJ (1994) The contribution of GABAA and glycine receptors to central sensitization: disinhibition and touch-evoked allodynia in the spinal cord. J Neurophysiol 72:169–179.

Song XJ, Wang ZB, Gan Q, Walters ET (2006) cAMP and cGMP contribute to sensory neuron hyperexcitability and hyperalgesia in rats with dorsal root ganglia compression. J Neurophysiol 95:479–492.

Sung YJ, Chiu DT, Ambron RT (2006) Activation and retrograde transport of protein kinase G in rat nociceptive neurons after nerve injury and inflammation. Neuroscience 141:697–709.

Tao F, Tao YX, Zhao C, Doré S, Liaw WJ, Raja SN, Johns RA (2004) Differential roles of neuronal and endothelial nitric oxide synthases during carrageenan-induced inflammatory hyperalgesia. Neuroscience 128:421–430.

Tao YX, Johns RA (2002) Activation and up-regulation of spinal cord nitric oxide receptor, soluble guanylate cyclase, after formalin injection into the rat hind paw. Neuroscience 112:439–446.

Tao YX, Hassan A, Haddad E, Johns RA (2000) Expression and action of cyclic GMP-dependent protein kinase Ialpha in inflammatory hyperalgesia in rat spinal cord. Neuroscience 95:525–533.

Tegeder I, Del Turco D, Schmidtko A, Sausbier M, Feil R, Hofmann F, Deller T, Ruth P, Geisslinger G (2004) Reduced inflammatory hyperalgesia with preservation of acute thermal nociception in mice lacking cGMP-dependent protein kinase I. Proc Natl Acad Sci U S A 101:3253–3257.

Tjølsen A, Berge OG, Hunskaar S, Rosland JH, Hole K (1992) The formalin test: an evaluation of the method. Pain 51:5–17.

Woolf CJ (2004) Pain: moving from symptom control toward mechanism-specific pharmacologic management. Ann Intern Med 140:441–451.

Zhang X, Chen Y, Wang C, Huang LY (2007) Neuronal somatic ATP release triggers neuron-satellite glial cell communication in dorsal root ganglia. Proc Natl Acad Sci U S A 104:9864–9869.

Zhuang ZY, Gerner P, Woolf CJ, Ji RR (2005) ERK is sequentially activated in neurons, microglia, and astrocytes by spinal nerve ligation and contributes to mechanical allodynia in this neuropathic pain model. Pain 114:149–159.

Zhuo M, Hu Y, Schultz C, Kandel ER, Hawkins RD (1994) Role of guanylyl cyclase and cGMP-dependent protein kinase in long-term potentiation. Nature 368:635–639.